CBETA as an ICS Source of Hard X-Rays

Kirsten Deitrick
For the CBETA ICS team

The Cockcroft Institute of Accelerator Science and Technology

MANCHESTER 1824 The University of Manchester

Old Dominion University

Jefferson Lab

Brookhaven National Laboratory — a passion for discovery

Office of Science — U.S. Department of Energy

Cornell Laboratory for Accelerator-based Sciences and Education (CLASSE)

UKRI Science and Technology Facilities Council

Outline

- Introduction
- Inverse Compton Scattering (ICS)
- Parameter Optimization and CBETA ICS Parameters
- ICS Bypass Design and Spectral Output
- Source Comparison
- Applications
- Spin-off Designs
- Conclusion

ICS Collaboration

Kirsten Deitrick[1], Georg Hoffstaetter[1], Carl Franck[1], Bruno D. Muratori[2], Peter H. Williams[2], Geoffrey A. Krafft[3,4], Balša Terzić[4], Joe Crone[5], Hywel Owen[5]

(1) Cornell University (2) STFC Daresbury Lab and Cockcroft Institute
(3) Jefferson Lab (4) Old Dominion University
(5) University of Manchester and Cockcroft Institute

Cornell Laboratory for Accelerator-based Sciences and Education (CLASSE)

Science and Technology Facilities Council

MANCHESTER 1824 The University of Manchester

OLD DOMINION UNIVERSITY

Jefferson Lab Thomas Jefferson National Accelerator Facility

The Cockcroft Institute of Accelerator Science and Technology

Some material taken from prior presentations by K. Deitrick and J. Crone

Introduction

- CBETA stands for Cornell-BNL ERL Test Accelerator

- Multi-turn SRF Energy Recovery Linac utilizing a non-scaling Fixed Field Alternating-gradient (FFA) permanent magnet return loop
  - Configuration of 1 - 4 turns with a maximum energy of 150 MeV

- FFA return loop has a wide energy acceptance – all 4 energies in the same pipe

- ERLs are characterized by the acceleration and deceleration of a bunch with the same SRF linac; the energy recovered by the deceleration is used to accelerate subsequent bunches

CBETA: Four-Turn Configuration

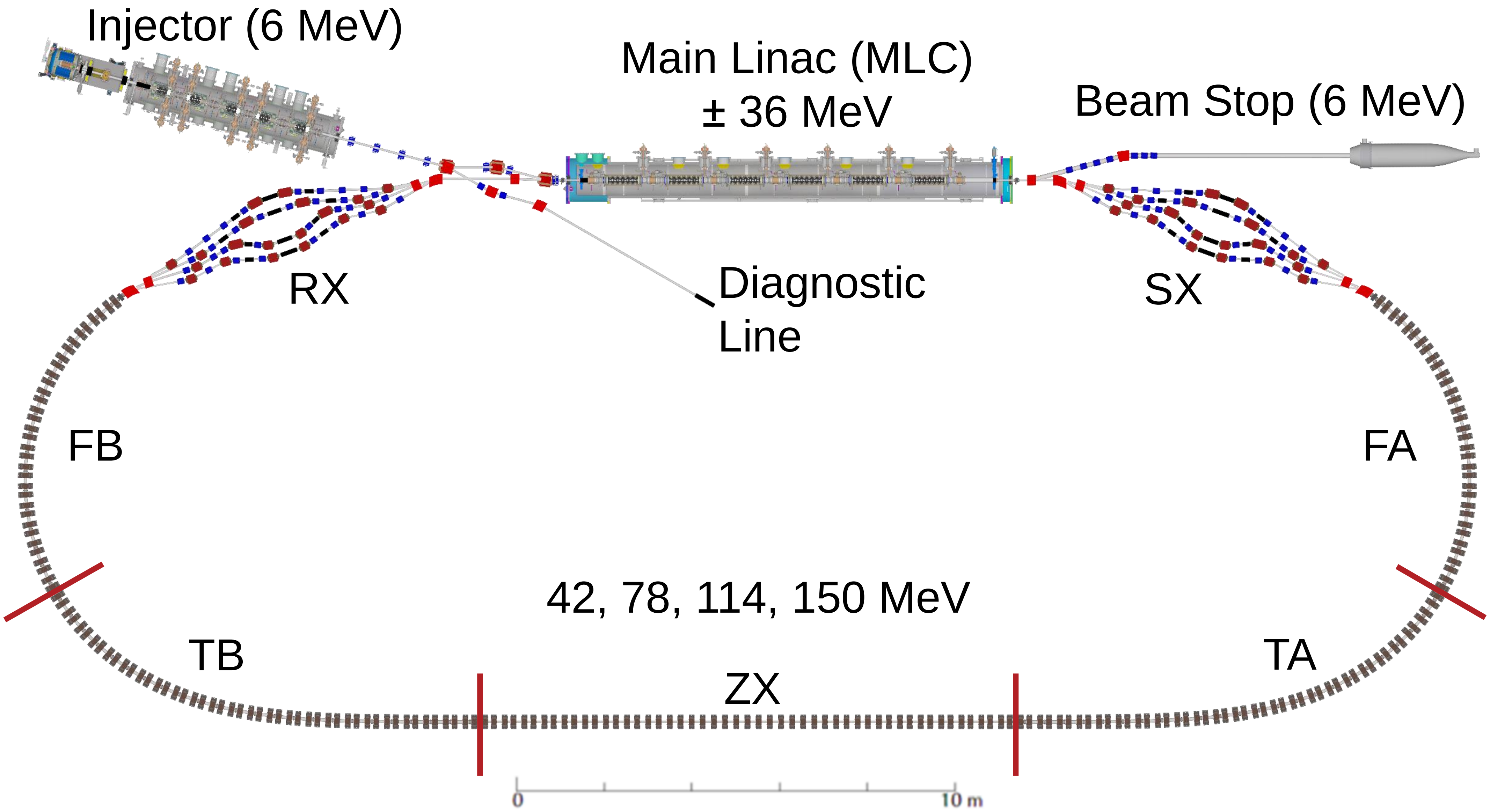

Inverse Compton Scattering (ICS)

- Collision of electron and photon at the interaction point (IP) produces radiation
- Energy of scattered radiation is given by

$$E_\gamma = \frac{E_{\text{laser}}(1-\beta\cos\phi')}{1-\beta\cos\theta+(1-\cos\theta')E_{\text{laser}}/E_e}$$

$$\phi' = \pi, \theta = 0$$

$$E_\gamma = \frac{4\gamma^2 E_{\text{laser}}}{1+X}$$

$$X = 4\gamma E_{\text{laser}}/m_e c^2$$

- Because E_γ is proportional to θ, a collimator can be used for energy selection and bandwidth control

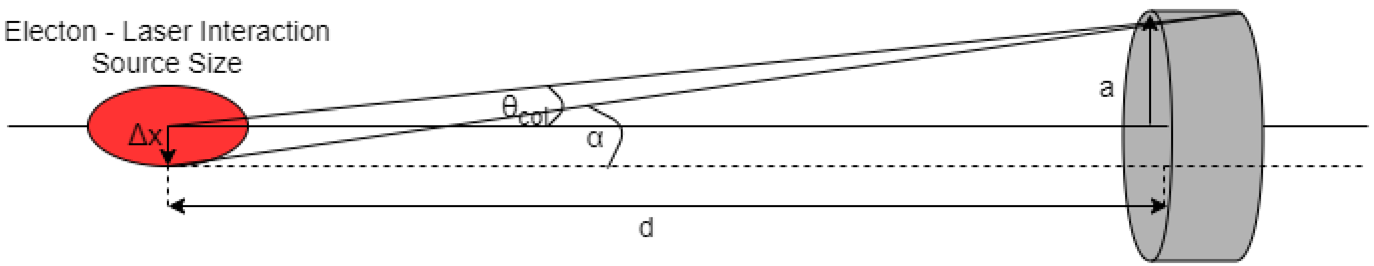

Schematic of an inverse Compton source with the laser – electron convolution source size and a downstream collimator for energy selection.

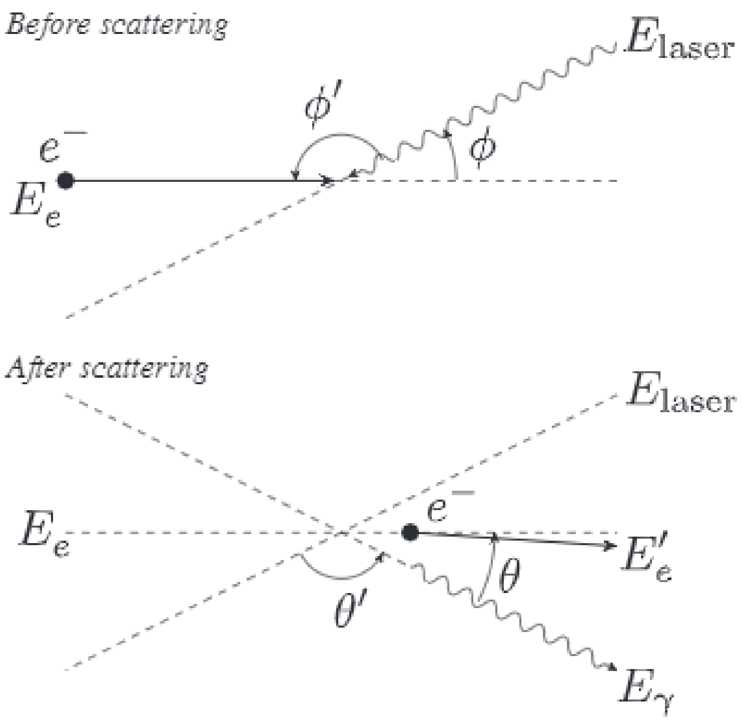

Scattering geometry of an inverse Compton scattering source. The angle ϕ is the crossing angle between the laser pulse and electron bunch and the angle θ is the angle between the scattered photons and the incident electron beam.

Inverse Compton Scattering

- Undulators typically have greater flux and brilliance for a given x-ray energy

- But:
  - Cost more
  - Bigger footprint
  - Limited availability
  - Higher energy spread x-rays

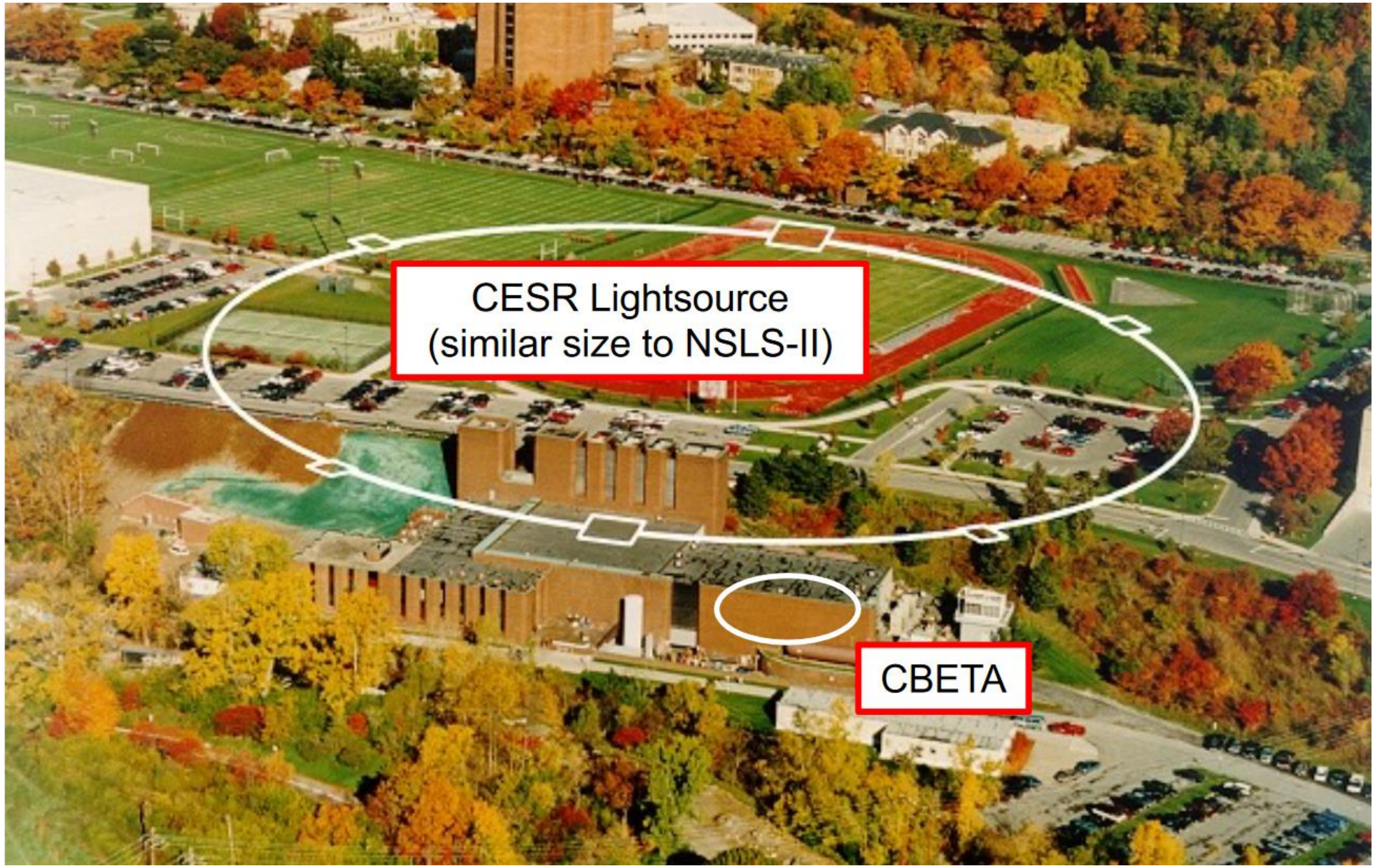

Picture from DOI: 10.18429/JACoW-IPAC2022-TUIZGD1

Parameter Optimization

- Optimization of bandwidth against collimated flux is performed by adjusting β at the IP and the collimation angle
- Collimated flux

$$\mathcal{F}_\Psi \propto \frac{\left(1+\sqrt[3]{X}\Psi^2/3\right)\Psi^2}{\left[1+(1+X/2)\Psi^2\right](1+\Psi^2)}$$

- Bandwidth of scattered radiation

$$\frac{\Delta E_\gamma}{E_\gamma} = \sqrt{\left(\frac{\sigma_\theta}{E_\theta}\right)^2 + \left(\frac{\sigma_e}{E_e}\right)^2 + \left(\frac{\sigma_L}{E_L}\right)^2 + \left(\frac{\sigma_\epsilon}{E_\epsilon}\right)^2}$$

- Minimum bandwidth

$$\lim_{\substack{\theta_{\mathrm{col}}\to 0 \\ \beta^*_{x/y}\to\infty}} (\Delta E_\gamma/E_\gamma) = \sqrt{\left(\frac{2+X}{1+X}\frac{\Delta E_e}{E_e}\right)^2 + \left(\frac{1}{1+X}\frac{\Delta E_L}{E_L}\right)^2}$$

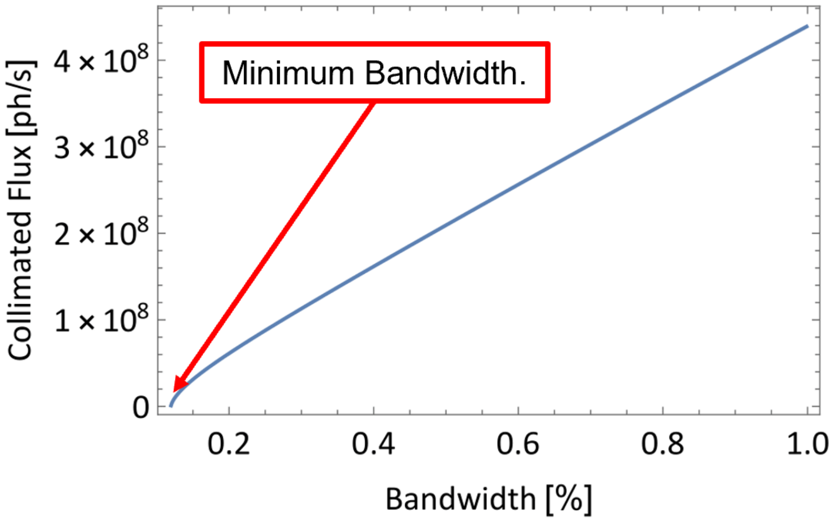

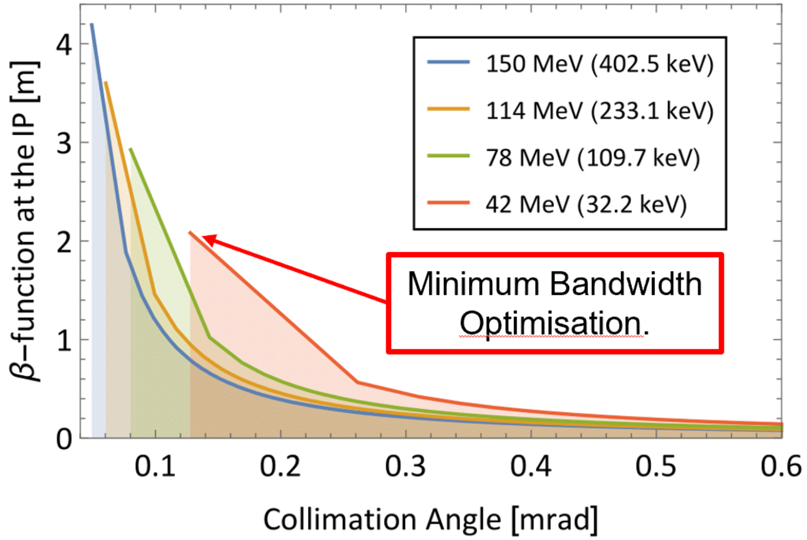

Top: CBETA ICS 150 MeV collimated flux – *rms* bandwidth round beam tuning curve. Recoil is small, so identical for all passes. Bottom: CBETA ICS $\theta_{col} - \beta^*$ parameter space displaying pareto front of optimised settings.

CBETA ICS Parameters

Top:

Laser pulse parameters at the IP, based on demonstrated 10 kW Nd:YAG optical cavity at cERL.

Bottom:

Electron beam parameters at the IP.

Parameter	Quantity	Unit
Wavelength, λ_{laser}	1064	nm
Photon energy, E_{laser}	1.17	eV
Pulse energy	62	μJ
Number of photons, N_{laser}	3.3×10^{14}	
Repetition rate, f	162.5	MHz
Spot size at the IP, σ_{laser}	25	μm
Crossing angle, ϕ	5°	
Pulse length	10	ps
Relative energy spread, $\Delta E_{laser}/E_{laser}$	6.57×10^{-4}	

Parameter	Quantity				Unit
Turn number	1	2	3	4	
Electron kinetic energy, E_e	42	78	114	150	MeV
Repetition rate, f			162.5		MHz
Bunch charge, eN_e			32		pC
Transverse normalised *rms* emittance, ϵ_N			0.3		mm-mrad
rms bunch length, $\Delta\tau$			1.0 (3.33)		mm (ps)
Relative energy spread			5.0×10^{-4}		
Baseline parameters					
β^* (at the IP)			1		cm
Electron bunch spot size, $\sigma_{electron}$	6.01	4.42	3.65	3.19	μm
Optimised for 0.5% (narrow) bandwidth					
β^* (at the IP)	3.56	6.58	9.60	12.62	cm
Electron bunch spot size, $\sigma_{electron}$	11.34	11.34	11.34	11.34	μm
Collimation angle, θ_{col}	1.533	0.830	0.569	0.433	mrad

ICS Bypass Design: CBETA Layout

- As is, there’s no room in the FFA for the interaction
- Assume linear magnets
- Not allowed to take out existing structures
- Using 150 MeV electrons

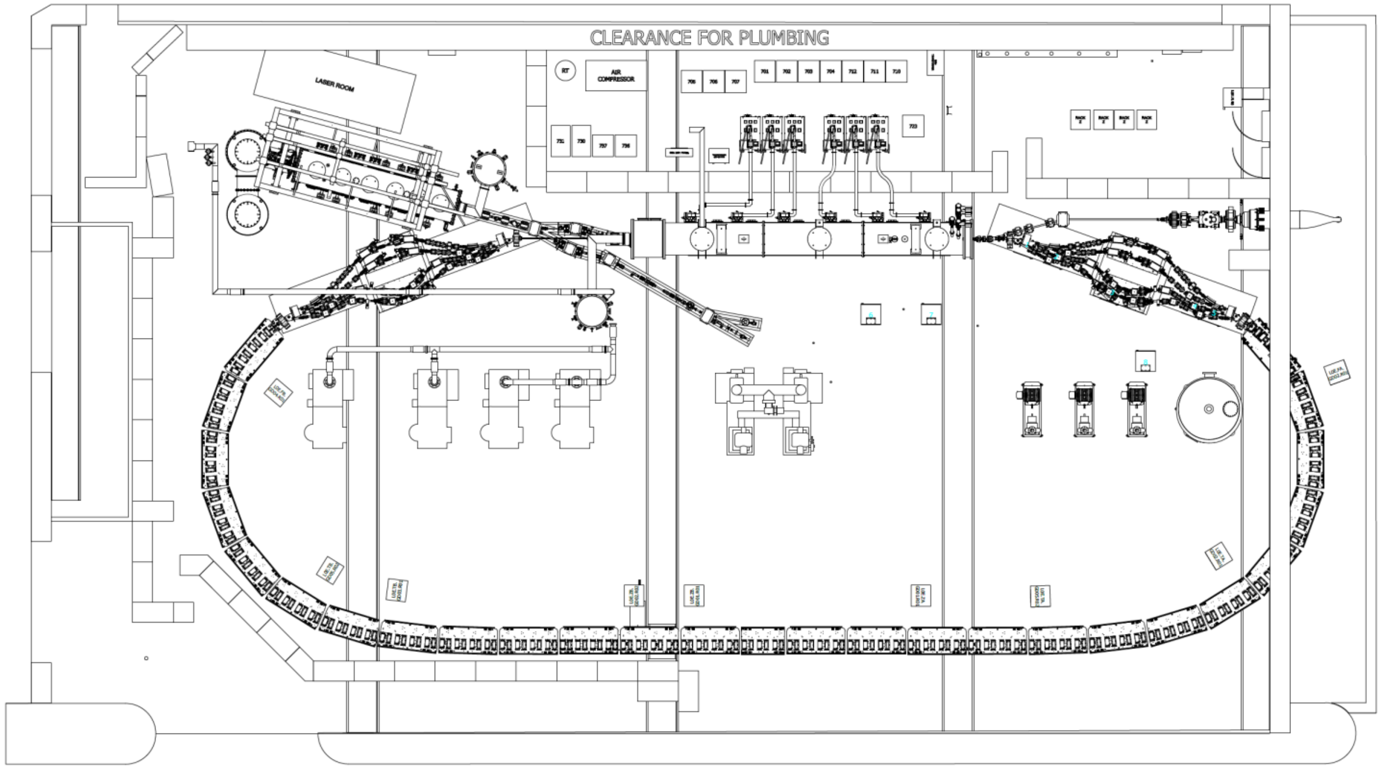

Schematic of the CBETA enclosure. MLC ~10 m for scale.

ICS Bypass Design: Overview

- Bypass line is elevated above existing plane by 30 cm; IP is further elevated by another 50 cm
- Optics are set such that the parameters going into the MLC for the fifth pass match CBETA design parameters

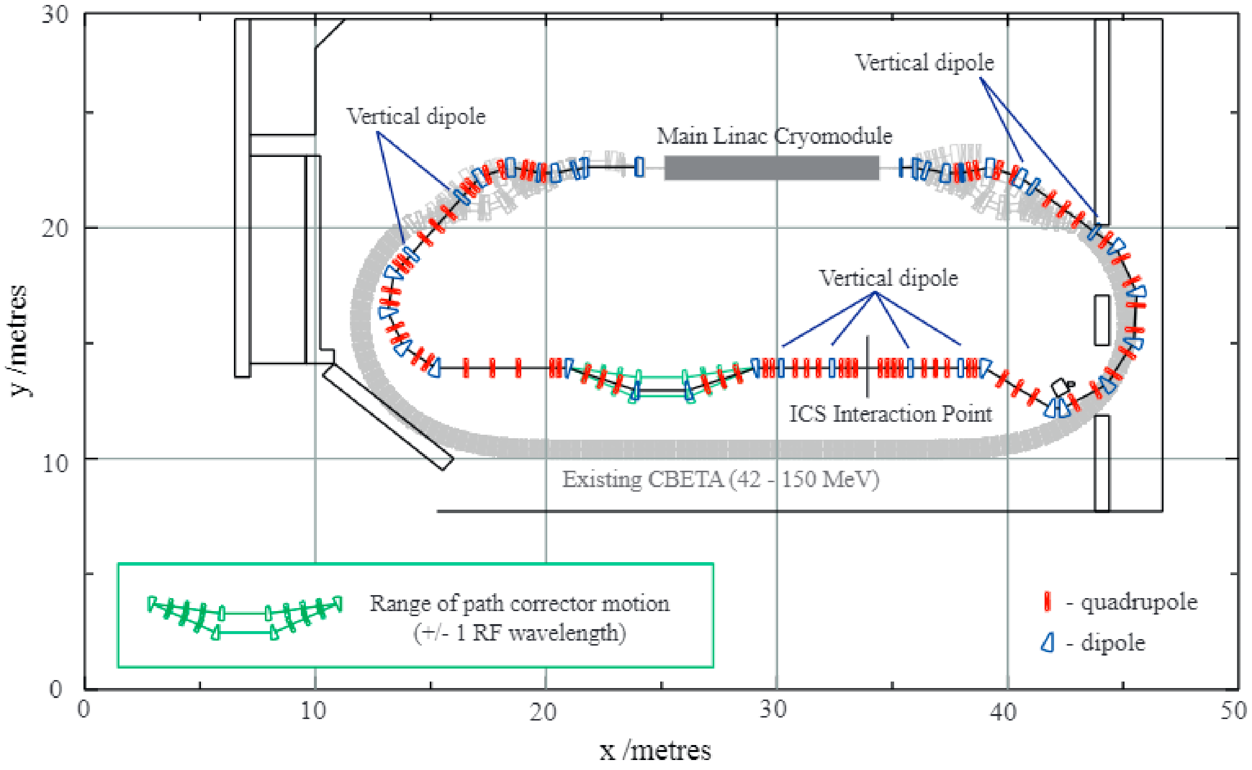

Floor plan schematic of the ICS bypass to CBETA. The existing CBETA return loop is shown in grey. The configurations of the path length correction system are shown in green. Vertical dipoles are indicated.

ICS Bypass Design: Path Length

- Bypass line removes the moving stages from S4/R4 – a new path length adjustment system is necessary

- Originally designed by H. Owen and P.H. Williams, this has a correction range of $\pm\lambda_{RF}$

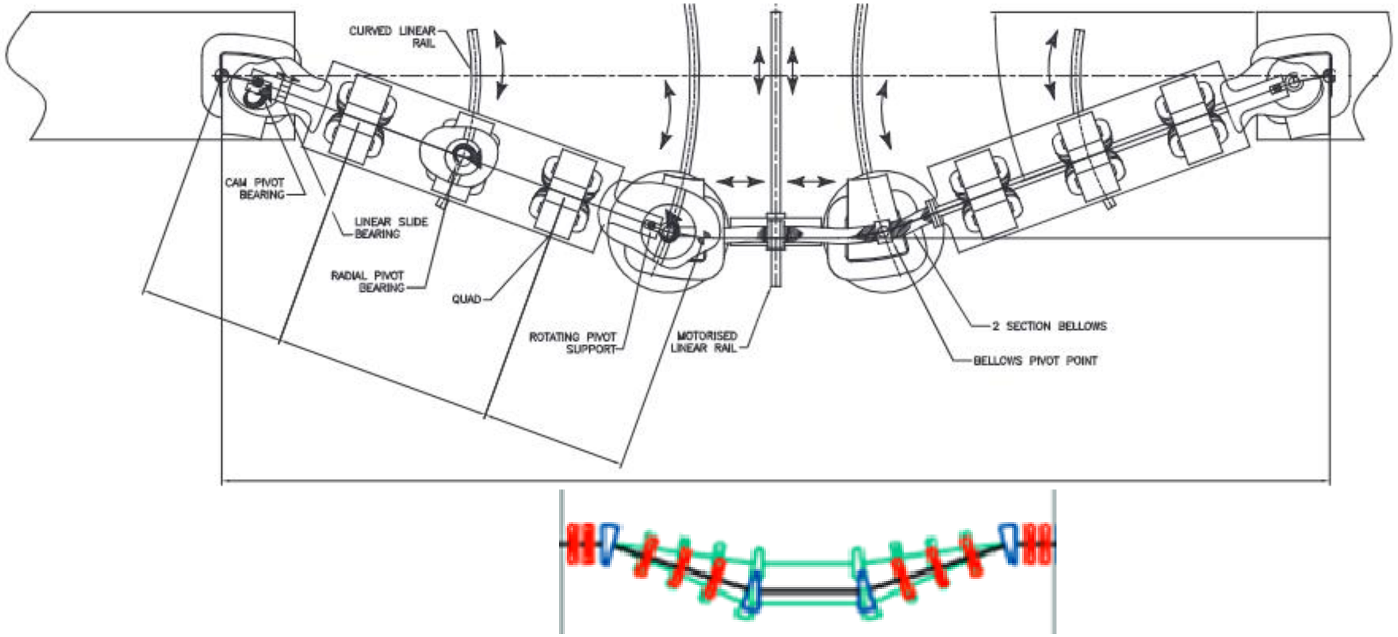

Schematic of the focusing chicane from the modular path length corrector design by H. Owen and P. Williams against the ICS bypass path length correction focusing chicane. Modified here for implementation into the CBETA bypass but retaining the same form.

ICS Bypass Design: Optics

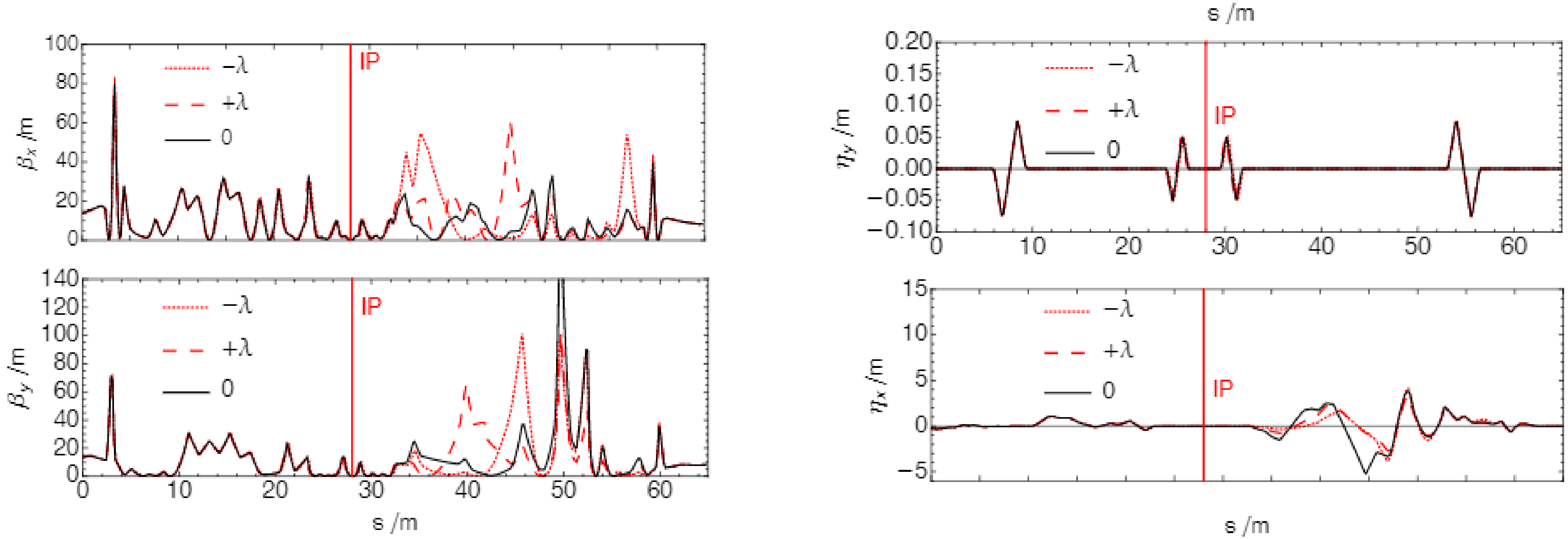

Left: β-function plots for the bypass lattice. Right: Dispersion plots for the bypass lattice. The solutions for the varying path length of -λ_{RF} (red, short dash), +λ_{RF}(red, long dash) and nominal (black, solid) are shown. IP is indicated in each plot by a red vertical line.

- $\beta_{x,y}^{peak}$ < 150 m – comparable to CBETA design
- $\beta_{x,y}$ at the IP sufficiently adjustable (0.01 – 0.126 m)
- Vertical dispersion is closed, horizontal is large between IP and R4

Spectral Output

Right:
CBETA ICS 150 MeV spectra produced by ICARUS and ICCS3D for a 0.5% BW. Note spectra are for the head-on case and therefore the position of the Compton edge is at a marginally higher energy and spectral density is not reduced by the angular crossing.

Bottom:
Spectral output parameters of the CBETA ICS. Note the peak brilliance is for a head-on collision, not the design crossing angle .

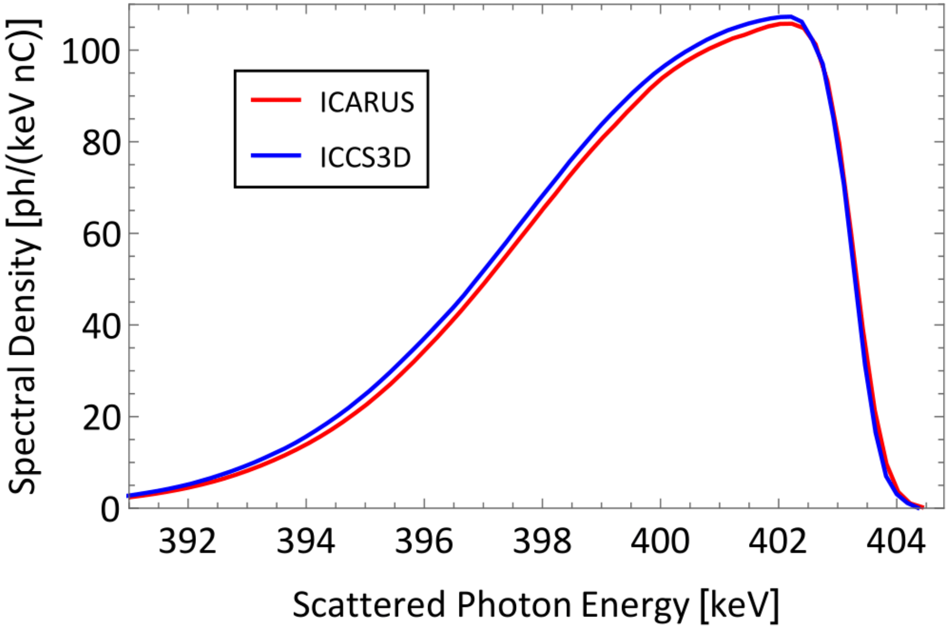

	Electron Kinetic Energy (MeV)				
	42	78	114	150	Unit
X-ray peak energy	32.2	109.7	233.1	402.5	keV
Uncollimated flux	3.16×10^{10}	3.20×10^{10}	3.21×10^{10}	3.22×10^{10}	ph/s
Spectral density	9.82×10^{5}	2.92×10^{5}	1.38×10^{5}	8.00×10^{4}	ph/s eV
Average brilliance	9.23×10^{10}	3.19×10^{11}	6.81×10^{11}	1.18×10^{12}	ph/s mm^2 mrad^2 0.1% bw
Peak brilliance	2.80×10^{15}	1.00×10^{16}	2.18×10^{16}	3.80×10^{16}	ph/s mm^2 mrad^2 0.1% bw
	0.5% bandwidth				
Collimated flux	2.09×10^{8}	2.09×10^{8}	2.09×10^{8}	2.09×10^{8}	ph/s 0.5% bw

Source Comparison: ICS

ICS	Accelerator type	Scattered photon energy (keV)	Flux (ph/s)
cERL [18]	ERL	6.95	2.6×10^7
ALICE [43]	ERL	21.5	9×10^5
MIT ICS[a] [44]	Linac	3–30	3×10^{14}
MuCLS [45]	Storage ring	15–35	$0.443 - 1.78 \times 10^{10}$
Tsinghua [46]	Linac	51.7	1×10^6
ThomX[a] [47]	Storage ring	45–90	$1 \times 10^{10} - 10^{13}$
BriXS[a] [48,49]	ERL	20–180	$1 \times 10^{10} - 10^{13}$
CBETA[a]	ERL	32.2, 109.7, 233.1, 402.5	$3.16 - 3.21 \times 10^{10}$
NIJI-IV [50]	Storage ring	1200	3.1×10^4
HIγS[b] [51]	Storage ring	1000–3000	5×10^7–5×10^8

[a]Denotes design parameters for sources which are not yet demonstrated.
[b]The HIγS source is capable of scattered photon energies from 1–100 MeV with varying fluxes (see Table V of Ref. [51]). Shown is the lowest energy operational setting, most comparable to the source presented here.

Operated ERL ICS sources.

Comparison of the CBETA ICS design against other designed ICS sources driven by differing forms of accelerator. Note that CBETA is competitive with all previously operated X-ray ICS sources, but flux is lower than some other designs due to conservative laser parameters. Shown in red are the two operated ERL driven ICS sources.

Source Comparison: Synchrotron

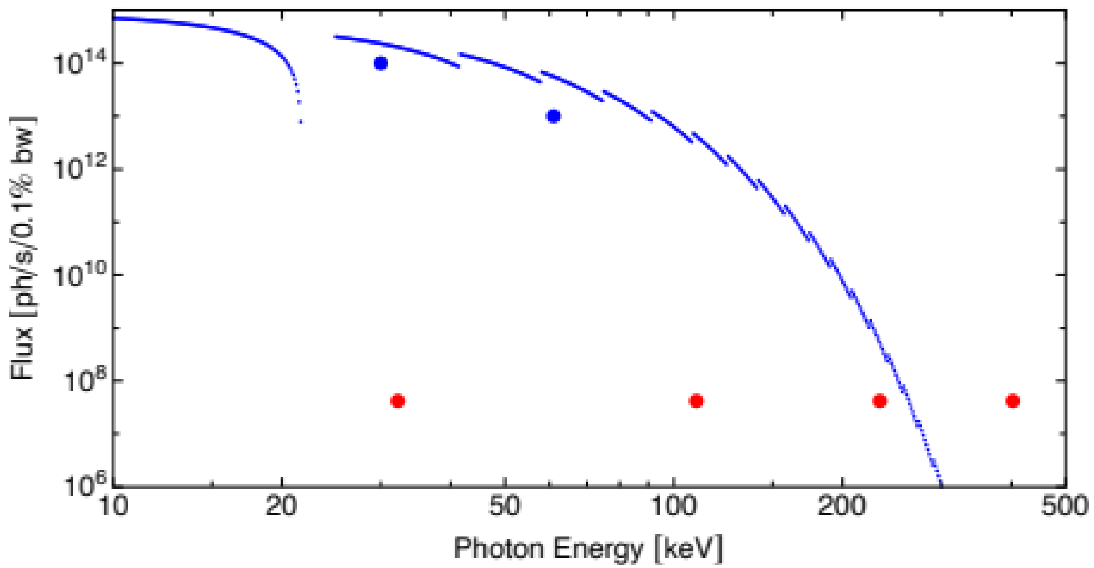

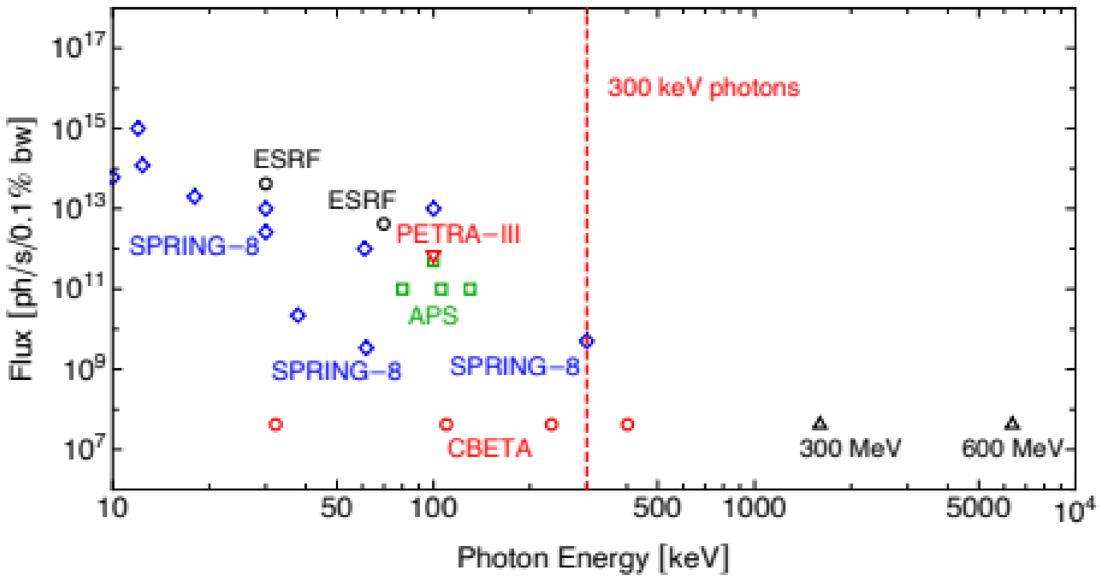

Left: Flux per 0.1% BW of the CBETA ICS (red) against the harmonic curves and data (blue) of the Spring-8 high energy undulator. Right: Flux per 0.1% BW of the CBETA ICS (red) against a collection of the major high energy storage ring undulators across the globe.

- Beyond ~300 keV, undulator radiation production is difficult due to high harmonics and undulator phase errors
- ICS footprint for MeV-scale γ-ray sources significantly smaller than synchrotron, while performing better

Applications

- X-ray fluorescence (XRF) of uranium and plutonium

- Energy-dispersive x-ray diffraction (EDXRD) – a high-flux source for identification of minerals in mined ore sample
  - High photon energy allows for inspection of thick samples

- Non-resonant inelastic x-ray scattering (NIXS) – high incident photon energy and large flux allows us to test materials such as transition metal oxides, which are a testbed for theories such as the Mott-Hubbard model

More Details…

PHYSICAL REVIEW ACCELERATORS AND BEAMS

Highlights Recent Accepted Special Editions Authors Referees Sponsors Search

Editors' Suggestion Open Access

Intense monochromatic photons above 100 keV from an inverse Compton source

Kirsten Deitrick, Georg H. Hoffstaetter, Carl Franck, Bruno D. Muratori, Peter H. Williams, Geoffrey A. Krafft, Balša Terzić, Joe Crone, and Hywel Owen

Phys. Rev. Accel. Beams **24**, 050701 – Published 27 May 2021

Article | References | No Citing Articles | PDF | HTML | Export Citation

Spin-off Design

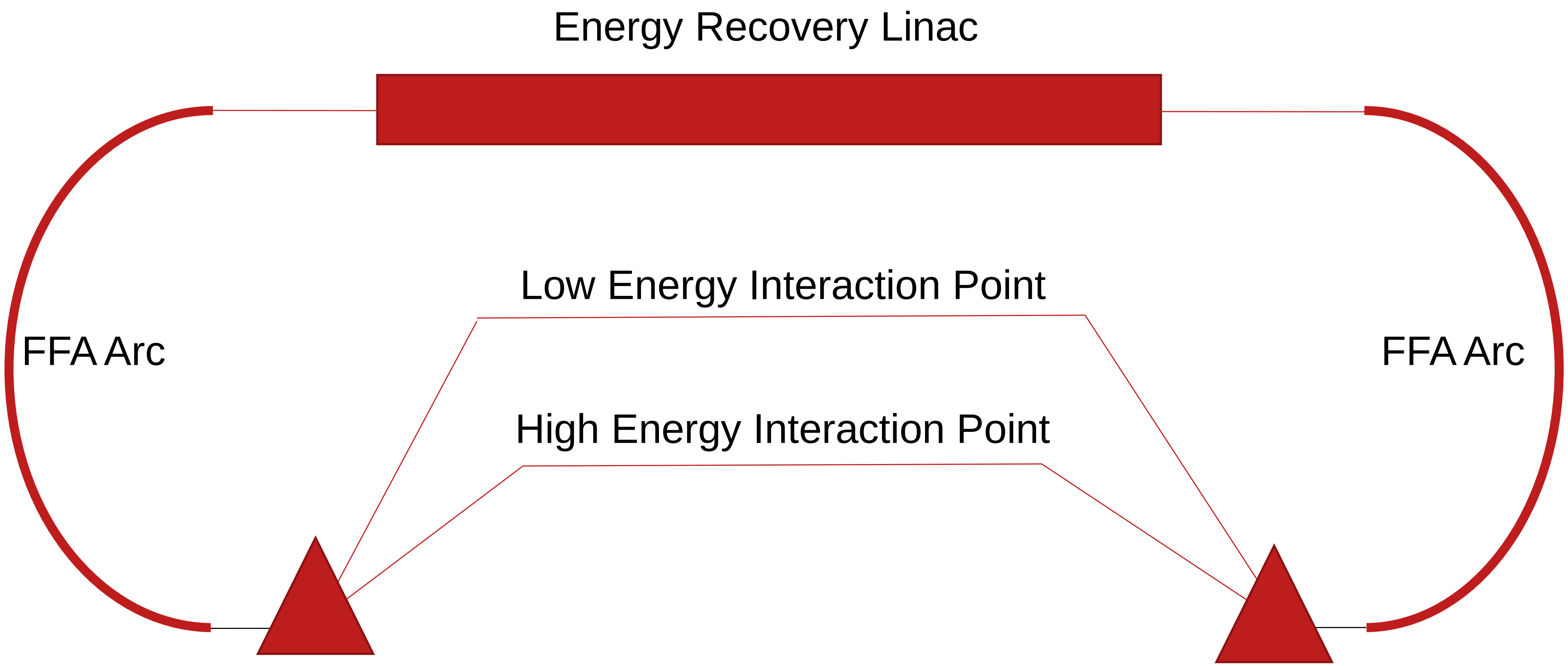

- Concept from Geoff Krafft (Jefferson Lab) for a simultaneous two-color Compton source

- Takes advantage of inherent wide-bandwidth in longitudinal direction

Spin-off Design

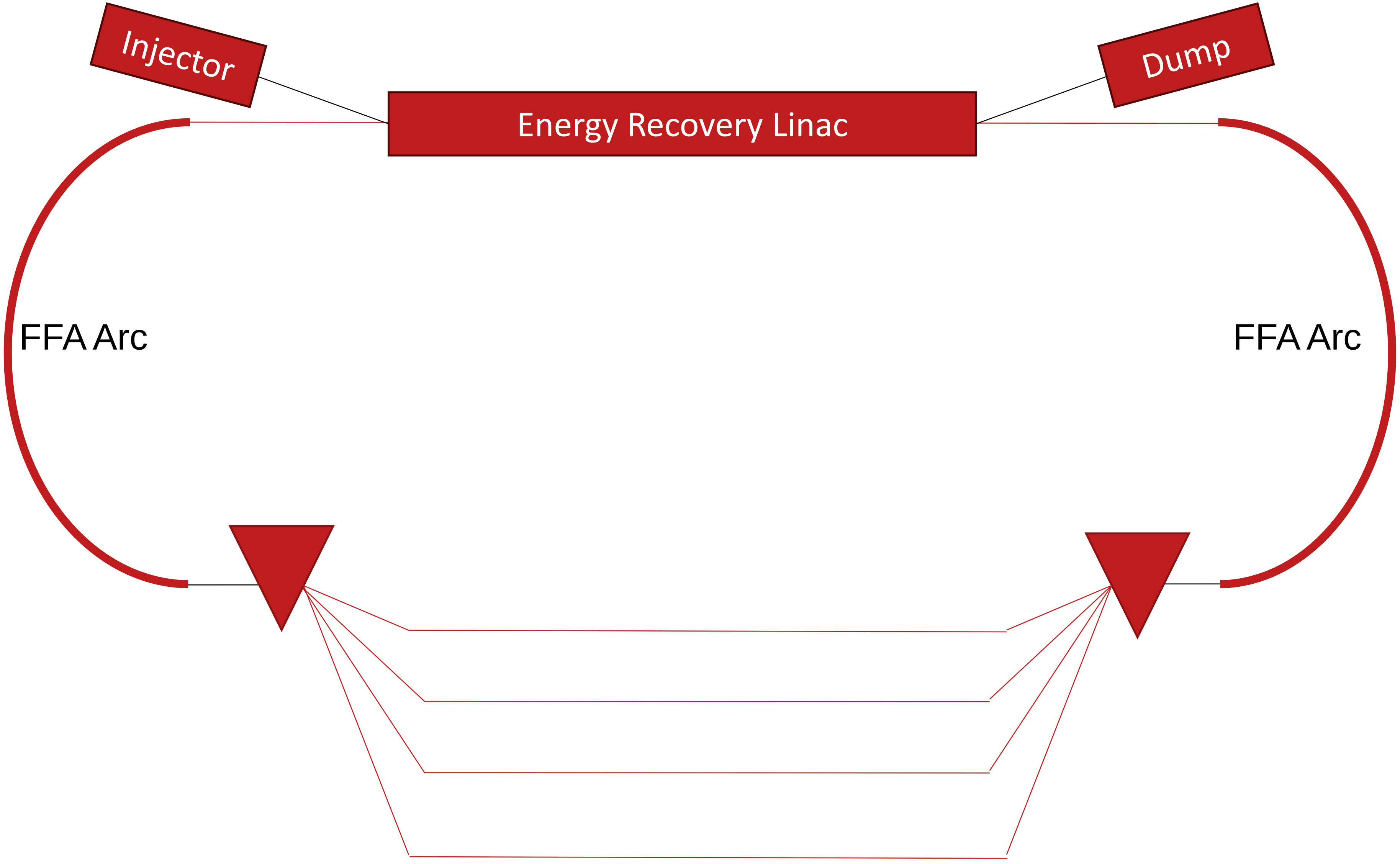

Conclusion

- ICS light sources have a variety of applications in a wide range of fields, including basic research, medical and industrial applications, cultural heritage, security, material science, and many more – x-ray usage is widespread

- CBETA ICS concept demonstrates both the suitability of an FFA ERL as an ICS-driver, while emphasizing that higher energy electron beams are capable of producing MeV-scale γ-rays in a relatively small footprint

- Hopefully, this inspires the development of FFA ERLs as light sources for the future

Questions?

Kirsten Deitrick

kirstend@jlab.org

Thanks for your attention!

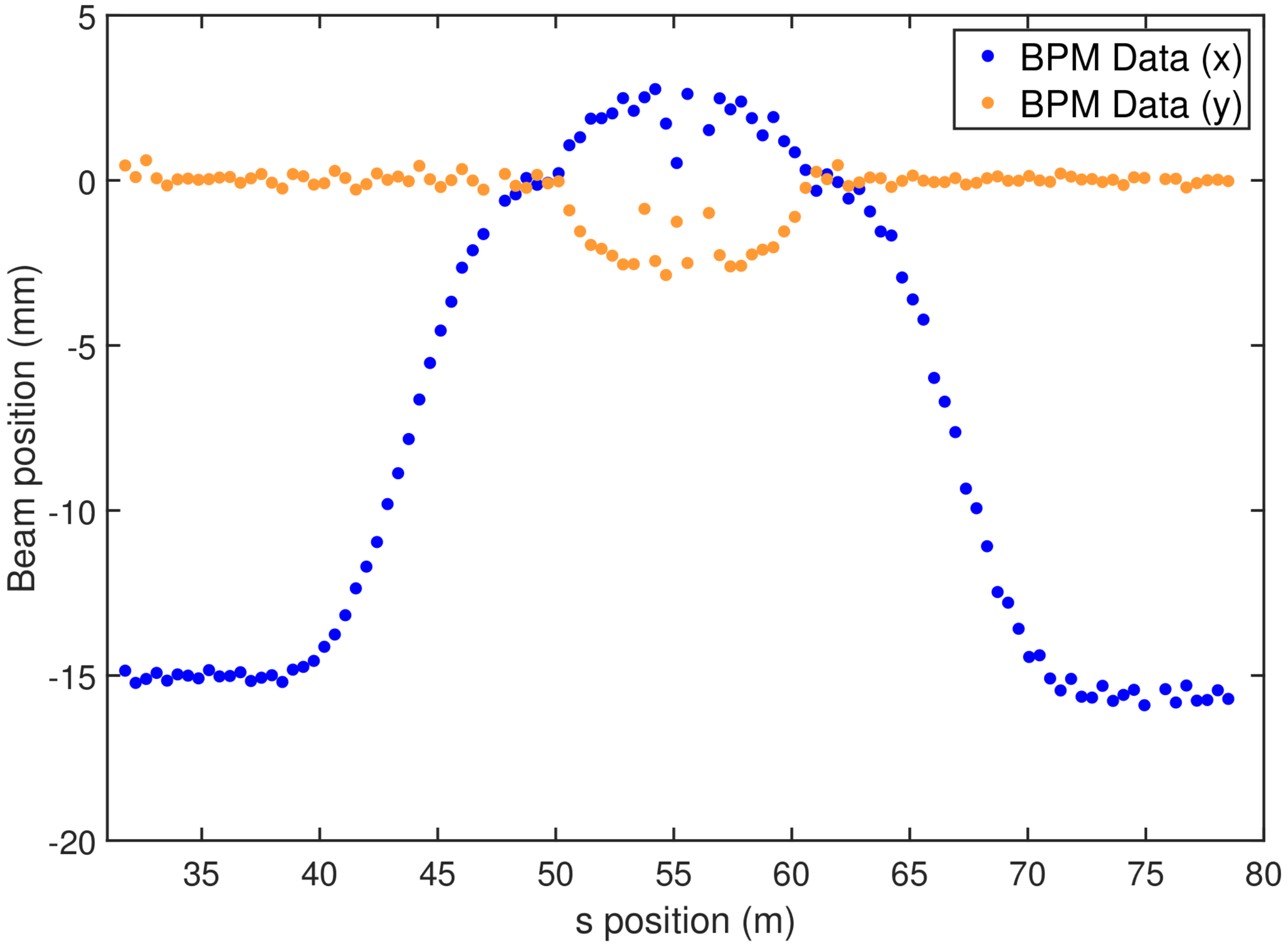

References

[18] T. Akagi, A. Kosuge, S. Araki, R. Hajima, Y. Honda, T. Miyajima, M. Mori, R. Nagai, N. Nakamura, M. Shimada, T. Shizuma, N. Terunuma, and J. Urakawa, Narrow-band photon beam via laser Compton scattering in an energy recovery linac, Phys. Rev. Accel. Beams **19**, 114701 (2016).

[43] G. Priebe, D. Laundy, P. Phillips, D. Graham, S. Jamison, S. Vassilev, E. Seddon, J. Rosenzweig, G. Krafft, T. Heinzl *et al.*, First results from the Daresbury Compton back-scattering x-ray source (cobald), in *Hard X-Ray, Gamma-Ray, and Neutron Detector Physics XII (International Society for Optics and Photonics* (2010), Vol. 7805, p. 780513, https://doi.org/10.1117/12.859671.

[44] W. S. Graves *et al.*, Compact x-ray source based on burst-mode inverse Compton scattering at 100 kHz, Phys. Rev. ST Accel. Beams **17**, 120701 (2014).

[45] E. Eggl, M. Dierolf, K. Achterhold, C. Jud, B. Günther, E. Braig, B. Gleich, and F. Pfeiffer, The Munich compact light source: Initial performance measures, J. Synchrotron Radiat. **23**, 1137 (2016).

[46] Y. Du, L. Yan, J. Hua, Q. Du, Z. Zhang, R. Li, H. Qian, W. Huang, H. Chen, and C. Tang, Generation of first hard x-ray pulse at Tsinghua Thomson scattering x-ray source, Rev. Sci. Instrum. **84**, 053301 (2013).

[47] K. Dupraz, M. Alkadi, M. Alves, L. Amoudry, D. Auguste, J.-L. Babigeon, M. Baltazar, A. Benoit, J. Bonis, J. Bonenfant *et al.*, The ThomX ICS source, Phys. Open **5**, 100051 (2020).

[48] P. Cardarelli, A. Bacci, R. Calandrino, F. Canella, R. Castriconi, S. Cialdi, A. Del Vecchio, F. di Franco, I. Drebot, M. Gambaccini *et al.*, BriXS, a new x-ray inverse Compton source for medical applications, Phys. Med. **77**, 127 (2020).

[49] I. Drebot *et al.*, Status of compact inverse Compton sources in Italy: BriXS and STAR, Proc. SPIE Int. Soc. Opt. Eng. **11110**, 14 (2019).

[50] N. Sei, H. Ogawa, and S. Okuda, Demonstration of narrow-band x-ray beam by inverse Compton scattering with stored spontaneous emission, J. Appl. Phys. **121**, 023103 (2017).

[51] H. R. Weller, M. W. Ahmed, H. Gao, W. Tornow, Y. K. Wu, M. Gai, and R. Miskimen, Research opportunities at the upgraded HIγS facility, Prog. Part. Nucl. Phys. **62**, 257 (2009).

Outline

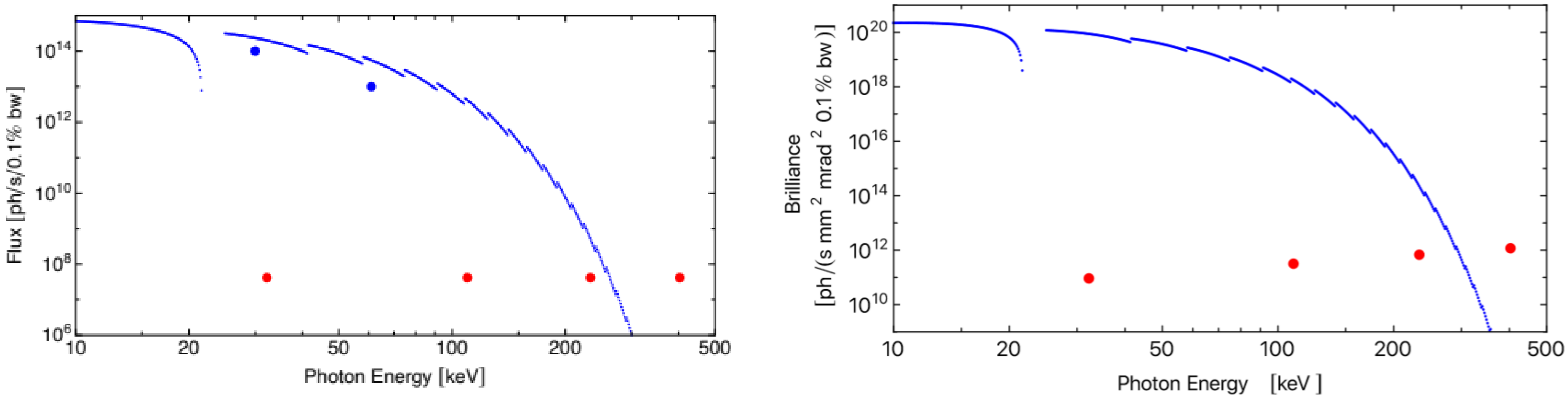

Comparison of CBETA predicted flux (left) and average brilliance (right) from the previous table with the output from a typical high-energy undulator – specifically, the BL10XU insertion at SPRING-8 (3rd generation source).